JOURNAL OF THERMOPHYSICS AND HEAT TRANSFER
Vol. 20, No. 4, October–December 2006

# Destabilization Mechanisms and Scaling Laws of Convective Boiling in a Minichannel

D. Brutin* and L. Tadrist†
*Ecole Polytechnique Universitaire de Marseille, 13453 Marseille, France*

DOI: 10.2514/1.15971

**Convective flow boiling in a minichannel is presently analyzed. A 889-m hydraulic diameter minichannel is used for the experiments conducted at several heat fluxes provided to the minichannel for variable inlet mass flow rates. A local analysis of the two-phase flow behavior through pressure and temperature measurements is detailed in the paper. Based on the flow boiling behavior, a destabilization mechanism is proposed on the vapor plug formation assumption. A theoretical criterion of the two-phase flow destabilization is proposed using a simplified model. The approach is compared with the experimental results. A scaling law is found with a nondimensional analysis of the experimental results.**

## Nomenclature

| | | |
|---|---|---|
| $A_H$ | = | area ($m^2$) |
| Bi | = | Biot number |
| $C$ | = | critical |
| $C_p$ | = | heat capacity ($J \cdot kg^{-1} \cdot K^{-1}$) |
| Co | = | confinement number |
| $D_H$ | = | hydraulic diameter (m) |
| $d$ | = | channel width (m) |
| $e$ | = | thickness (m) |
| $F$ | = | frequency (Hz) |
| $h$ | = | heat transfer coefficient ($W \cdot m^{-2} \cdot K^{-1}$) |
| $k$ | = | thermal conductivity ($W \cdot m^{-1} \cdot K^{-1}$) |
| $L$ | = | length (m) |
| $L_C$ | = | location in the channel where the flow stops (m) |
| $L_V$ | = | latent heat of vaporization ($J \cdot kg^{-1}$) |
| $l$ | = | width (m) |
| $m$ | = | mean |
| $N_{\text{pch}}$ | = | phase change number |
| $N_{\text{sub}}$ | = | subcooling number |
| $P$ | = | pressure (Pa) |
| $Po$ | = | Poiseuille number |
| $Re$ | = | Reynolds number |
| $T$ | = | temperature (°C) |
| TP | = | tow phase |
| $U$ | = | velocity ($m \cdot s^{-1}$) |
| $V$ | = | vapor |
| $z$ | = | location along the channel (m) |
| 0 | = | entrance |
| $\alpha$ | = | Poiseuille number |
| $\Delta$ | = | difference |
| $\lambda$ | = | friction factor |
| $\mu$ | = | dynamic viscosity ($Pa \cdot s$) |
| $\varrho$ | = | density ($kg \cdot m^{-3}$) |
| $\sigma$ | = | surface tension ($N \cdot m^{-1}$) |
| $\chi$ | = | vapor quality |

*Subscripts*

| | | |
|---|---|---|
| in | = | inlet |
| out | = | outlet |

Received 6 February 2005; revision received 22 October 2005; accepted for publication 4 November 2005. Copyright © 2005 by the American Institute of Aeronautics and Astronautics, Inc. All rights reserved. Copies of this paper may be made for personal or internal use, on condition that the copier pay the $10.00 per-copy fee to the Copyright Clearance Center, Inc., 222 Rosewood Drive, Danvers, MA 01923; include the code $10.00 in correspondence with the CCC.

*Research Assistant Professor, Laboratoire IUSTI Technopôle de Château–Gombert 5, rue Enrico Fermi; david.brutin@polytech.univ-mrs.fr (corresponding author).

†Professor, Laboratoire IUSTI Technopôle de Château–Gombert 5, rue Enrico Fermi.

## I. Introduction

UNSTEADY flows are often encountered when boiling occurs in small channels [1–3]. We analyzed in Table 1 a few studies dealing with unsteady flows and flow boiling instabilities in mini- and microchannels [20,21]. This phenomenon is related to the confined effects on bubble behavior in the microducts. Yan and Kenning [12] observed high surface temperature fluctuations for a minichannel of 1.33 mm-hydraulic diameter. Surface temperature fluctuations (1 to 2°C) were deduced from gray level fluctuation of liquid crystals. The authors evidenced a coupling between the flow and heat transfer by obtaining the same fluctuations frequencies between the surface temperature and two-phase flow pressure fluctuations.

Kennedy et al. [15] studied convective boiling in circular minitubes of 1.17 mm in diameter using distilled water and focused on the nucleation boiling and unsteady flow thresholds. They obtained experimentally these thresholds by analyzing pressure losses curves function of inlet mass flow rate for several heat fluxes. They deduced from their observations the heat flux under which flow boiling becomes unsteady (90% of the heat flux necessary for a full fluid vaporization). A relation between these two parameters seems to exist, however, the choice of the 90% by the authors is not clear.

Qu and Mudawar [18] evidenced two kinds of unsteady flow boiling: either a spatial global fluctuation of all the two-phase zone for all the microchannels or anarchistic fluctuations of the two-phase zone: overpressure in one microchannel and underpressure in another. These coupling phenomena between microchannels were predictable because of a plenum before the microchannels' entrance. The individual microchannel mass flow rate is not controlled. To avoid such a situation it is important to have a constant mass flow rate at each microchannel entrance.

In a previous paper, we detailed the experimental setup (Figs. 1 and 2) designed to analyze convective boiling in minichannels [20]. The loop is composed of a minichannel, an injection device (hydraulic jack coupled to an engine), which allows to provide a constant mass flow rate. A fluid storage volume is introduced before the minichannel entrance. The local instrumentation allows one to access the local pressure and temperature measurements, whereas the fast recording camera allows one to observe and analyze the flow patterns of steady and unsteady regimes. A study of the inlet flow condition on the two-phase flow stability evidenced a coupling between the minichannel and the injection device when a fluid storage volume is introduced before the minichannel entrance. The consequence is unsteady two-phase flow of high amplitude and low

**Table 1 Studies on boiling flow's instabilities in mini- and microchannels[a]**

| Authors, year [reference] | Fluid | Geometry | Field | Aim of the study |
|---|---|---|---|---|
| Stenning [4] | R-11 | —— | Exp | Flow oscillations observations |
| Davies [5] | —— | —— | Th | Coupled system stability |
| Bouré [6] | —— | —— | Exp | Review on liquid–vapor instabilities |
| Bergles [7] | —— | —— | Exp | Review on liquid–vapor flows |
| Blum [8] | —— | Circ | Th | Boiling flow linear stability analysis |
| Kew [9] | Water, R141b | Rect, Circ | Th and Exp | Two-phase flow modeling using vapor slug expansion |
| Chang [10] | Water | Rect | Th and Exp | Critical heat flux prediction |
| Umekawa [11] | Water | Circ | Exp and Num | Oscillating flow dryout modeling |
| Yan [12] | Water | Rect | Exp | Unsteady pressure and temperature meas in upward boiling flow |
| Kim [13] | Water | Circ | Exp | Stability influence on critical heat flux |
| Roach [14] | Water | Circ | Exp | Unsteady flow criteria study |
| Kennedy [15] | Water | Circ | Exp | Unsteady flow criteria study |
| Babelli [16] | R-113 | Ann | Th and Exp | Unsteady two-phase flow evidence |
| Peles [17] | Water | Tri | Th and Exp | 1-D modeling using Peclet and Jacob dimensionless numbers |
| Qu [18] | Water | Rect | Th and Exp | Coupling instabilities in parallel microchannels |
| Li [19] | Water | Tri | Exp | Unsteady flows observed for two parallel microchannels |

[a]Tri: triangular; rect: rectangular; circ: circular; ann: annular; th: theoretical; exp: experimental; num: numerical; meas: measurement.

frequencies appear compared with unsteady flow when no fluid storage volume exist [21].

## II. Physical Model

The confinement effect on boiling appears through the wall influence on the flow. In a large tube, boiling is not influenced by the wall's duct and the flow is free to structure and evolve inside. In our minichannel, dimensions are such as the bubble growth from a nucleation site is modified by the wall proximity (Fig. 3). A criteria is to verify the bubbles are larger than the duct diameter. We estimate the bubble detachment diameter using for *n*-pentane the correlation of Fritz [22] which takes into account nucleation surface orientation. We use Eq. (1) where $\theta$ is the wetting angle expressed in degrees. This relation is based on the balance between surface tension and buoyancy forces. We obtain a bubble detachment diameter of 600 $\mu$m; which means that inside our minichannel of 500 $\mu$m thickness, the wall proximity influences the bubble evolution. Thus, it is reasonable to think that wall confinement will influence the vapor bubble behavior and coalescence in the minichannel.

$$D_{\text{bubbles}} = 0.0208\theta\sqrt{\frac{\sigma}{g(\varrho_L - \varrho_G)}} \tag{1}$$

Now, we can consider that one liberty degree has been removed. The consequence is that bubbles will grow following the two other axes (width and length). Whereas bubbles are supposed to be spherical without influence of any wall, here there are compressed. This shape modification induces an increase of wall friction. Confinement increases the bubble coalescence by reducing the minichannel volume for a given surface; the bubble volumetric density quickly grows and thus bubble groups into slugs. Because of the wall proximity, the wall friction for bubbles and slugs evolution is increased. When vapor slugs flow through the minichannel, they

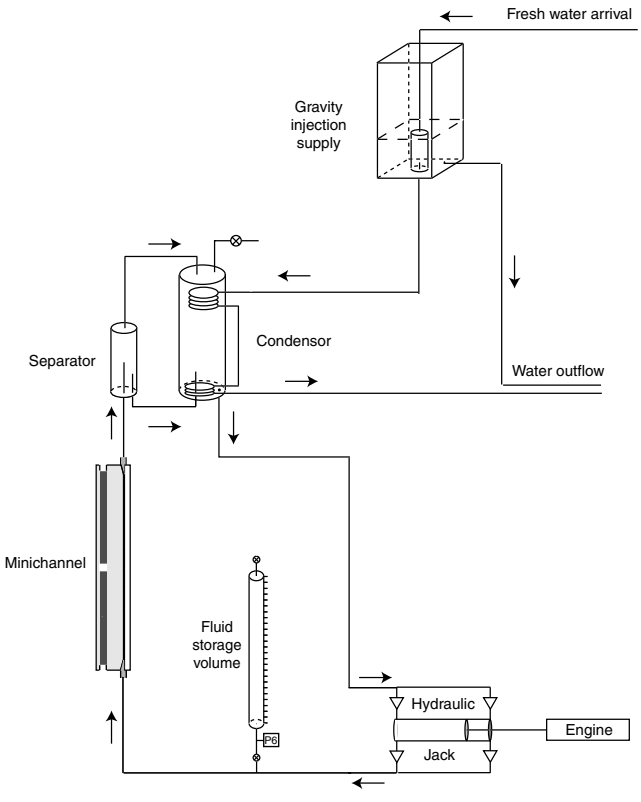


**Fig. 1 Complete experimental setup composed of the minichannel, the condensation system, the injection device.**

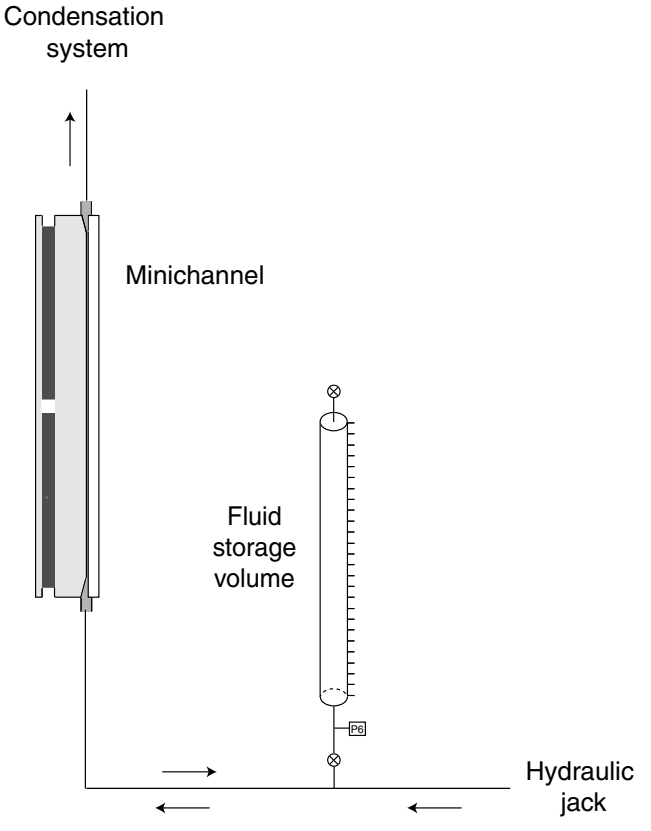


**Fig. 2 The coupling system with the minichannel studied and the fluid storage volume.**

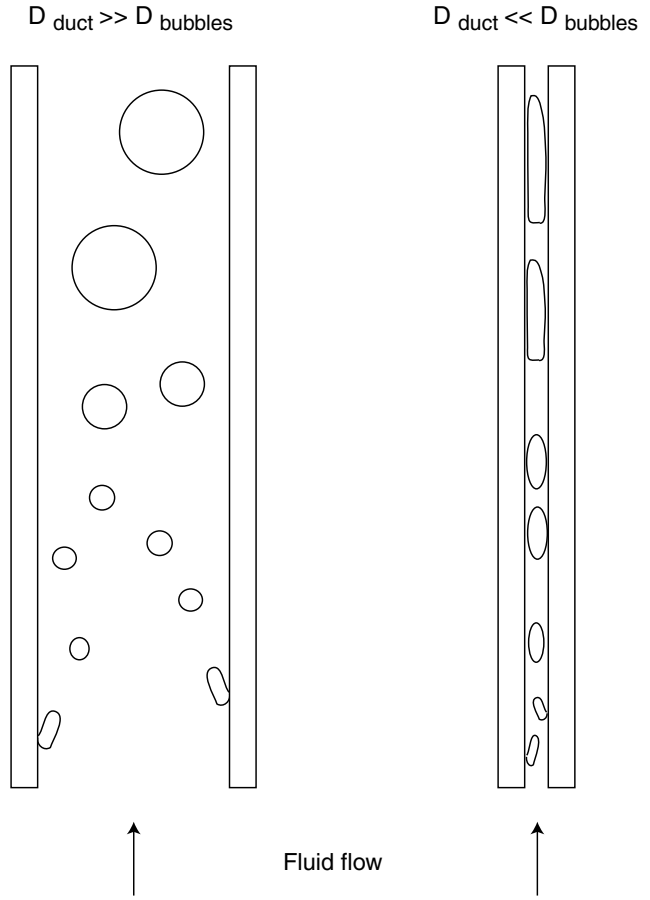


**Fig. 3 Wall influence on flow boiling behavior.**

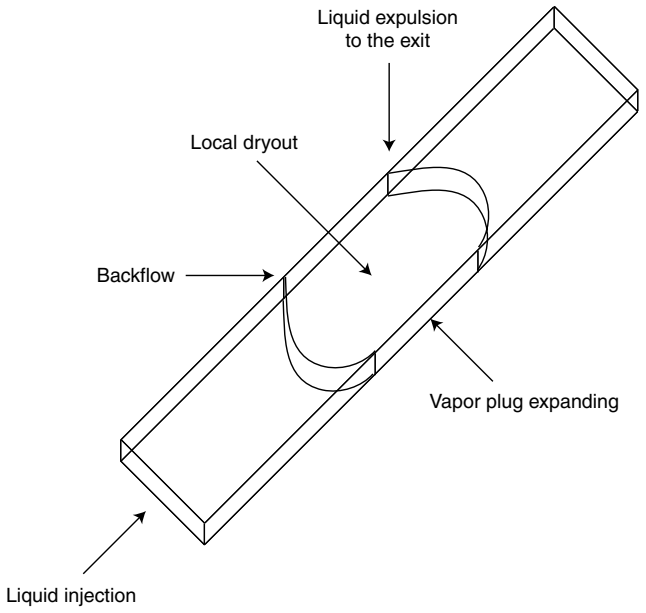


**Fig. 4 Local dryout due to a vapor slug.**

induce wall overheat due the heat transfer reduction associated with the vapor phase (Fig. 4). These periodical slugs are more and more numerous with heat flux increases or liquid mass flow rate decreases.

Slugs always appear in the first half of the minichannel. This has been confirmed by a detailed analysis of fast camera recording [23] (because a backflow behavior is possible due to the presence of a volume storage before the minichannel entrance, slug expansion is not symmetrical and the characteristic time of an unsteady period can be split into specific steps: the expulsion time and the refilling one).

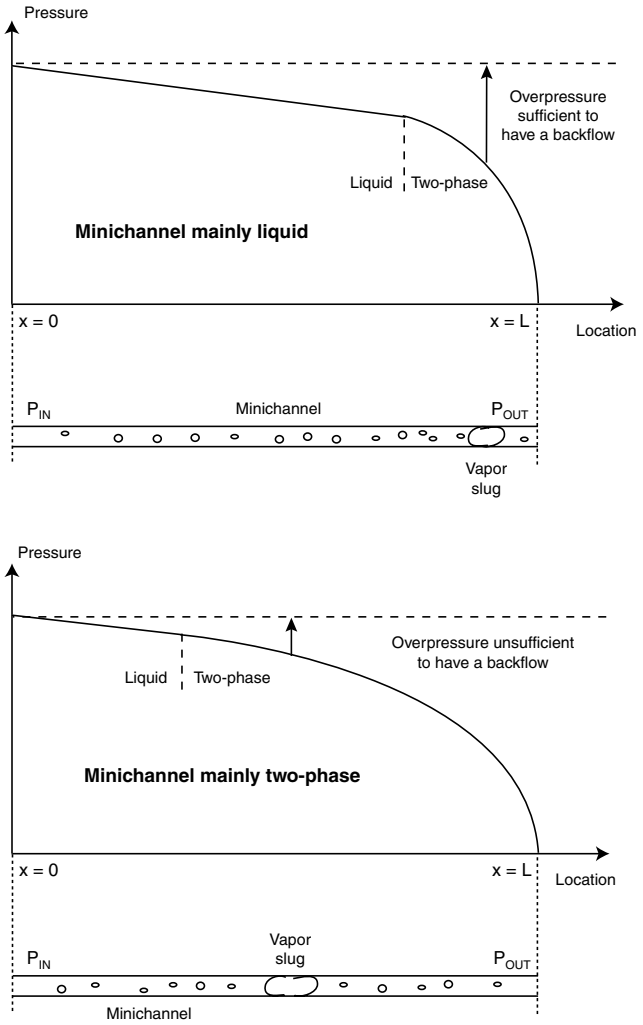


**Fig. 5 Local pressure in the minichannel for two situations: a flow mainly liquid and a flow mainly two-phase.**

To explain why slugs appear always in the first half of the minichannel, it is necessary to analyze and model the local pressure variation. The slug formation and displacement in the minichannel must be associated to local pressure variations. A backflow behavior can appear only if local pressure is higher compared with the entrance pressure. The slug formation which evolves more and more quickly in the minichannel induces local overpressures. If these overpressures occur fast enough compared with the time to transmit pressure through the two-phase medium, the fluid can flow back to the entrance. If the two-phase zone exists only at the exit of the minichannel (top of Fig. 5), overpressure must be important to have backflow because it has to be higher than the injection pressure. However, when boiling appears at the exit of the minichannel, vapor quality and void fraction are quite small, bubble flow does not create high amplitudes overpressures. If the two-phase zone is mainly present inside the minichannel (bottom of Fig. 5), flow is composed of slugs which evolve quickly. High two-phase overpressure increases locally over the injection pressure inducing a backflow behavior.

Considering the buffer tank connected before the minichannel entrance, when the backflow behavior phenomena occurs, part of the two-phase zone flows back to the entrance and another flows to the exit. The fluid which flows back to the entrance is stored in the buffer tank. Injection pressure is provided by the buffer which stores more and more fluid. As soon as the injection pressure is higher than the minichannel pressure loss, the buffer fluid and the fluid provided by the injection device can be reintroduced to refill the minichannel. The process can be repeated because the obstruction of minichannel conditions can be reproduced. The origins of the flow unsteady state

have been evidenced to come from the slug formation in the two-phase near the minichannel entrance. A model is proposed to predict the transition from steady to unsteady state. The model is based on the local pressure necessary to evacuate all the two-phase fluid inside the minichannel.

## III. Theoretical Stability Criterion

### A. Model Basis

Based on Fig. 5, we define $L_c$ the location in the minichannel where the flow stops, the slug expands to purge all that out of the minichannel. $U_0$ is the injection liquid velocity at the bottom of the minichannel, $\bar{U}$ the average two-phase flow evacuation velocity. Two terms have to be quantified: on one side we have to take into account the overpressure induced by the vapor slug expansion and on the other side we have to quantify injection pressure minus the minichannel outlet pressure. The pressure necessary to evacuate all the minichannel of fluid is mainly the minichannel pressure loss because the outlet pressure is above the atmospheric pressure. To estimate the friction pressure loss in the minichannel, we neglect the acceleration and gravity terms. The two-phase flow physical properties are considered to be the average between the inlet and the outlet. When unsteady states appear, we consider the fluid entered saturated. Thus, we can establish the overpressure expression ($\Delta P_{\text{slug}}$) to evacuate all the two-phase flow from the minichannel [Eq. (2)]. The flow regime considered just after the flow stops is laminar because this minimizes the energy used for the evacuation; a turbulent regime would necessitate much more enthalpy and thus the overpressure would be much higher. In the expression $\bar{\lambda} = \alpha/\bar{Re}$, we take $\alpha = 82.36$ for our geometry aspect ratio. The minichannel pressure loss is $\Delta P_{\text{minichannel}}$. Overpressure created by the vapor slug is scaled by the dynamic pressure $\frac{1}{2}\varrho_0 U_0^2$.

$$\Delta P_{\text{slug}} = \bar{\lambda}\frac{L}{D_H}\frac{\varrho_m U_m^2}{2} = \frac{\alpha L \bar{\nu}\varrho_m U_m}{2D_H^2} \tag{2}$$

$$\frac{\Delta P_{\text{slug}}}{\frac{1}{2}\varrho_0 U_0^2} = \bar{\lambda}\frac{L}{D_H}\frac{\bar{\varrho} U_m^2}{\varrho_0 U_0^2} = \frac{\alpha L \bar{\nu}\varrho_m U_m}{\varrho_0 U_0^2 D_H^2} \tag{3}$$

If the overpressure created by the vapor slug is higher to the minichannel pressure loss, the slug can grow and purge the minichannel. This condition can be written as Eq. (4) and in nondimensioned form as Eq. (5).

$$\Delta P_{\text{slug}} > \Delta P_{\text{minichannel}} \tag{4}$$

$$\frac{\Delta P_{\text{slug}}}{\frac{1}{2}\varrho_0 U_0^2} > K_1 \tag{5}$$

Thus, $K_1$ is the critical threshold to reach. Viscosity, density, and average velocity of the two-phase flow to purge have to be determined. The average vapor quality allows one to estimate the product between the density and average velocity of the two-phase flow. Thus, if we consider Eq. (6), the solution of the enthalpy equation gives Eq. (7). The heated perimeter $(d + 2e)$ will be designed in the future by $\delta$ for mathematical simplification purposes.

$$\varrho_0 U_0 L_V \frac{d\chi_V}{dz} = \frac{Q_W(d + 2e)}{A_H} \tag{6}$$

$$\chi_V(z) = \frac{Q_W \delta z}{A_H L_V \varrho_L U_L} \tag{7}$$

The average vapor quality ($\bar{\chi}_V$) is obtained by the continuous averaging of the vapor quality along the minichannel. It can also be defined as the ratio between the average vapor mass flow rate and the total liquid flow injected [Eq. (9)].

$$\bar{\chi}_v = \frac{1}{L}\int_{z=0}^{z=L} \chi_V(z)\, \mathrm{d}z = \frac{Q_W \delta L}{2A_H L_V \varrho_0 U_0} \tag{8}$$

$$\bar{\chi}_v = \frac{\bar{m}_V}{\dot{m}_0} = \frac{\varrho_m U_m}{\varrho_0 U_0} \tag{9}$$

$$\varrho_m U_m = \frac{Q_W \delta L}{2A_H L_V} \tag{10}$$

The average viscosity $\bar{\nu}$ is estimated from the Dukler correlation [Eq. (11)] for a homogeneous media. Using the average vapor quality, we deduce the average two-phase flow viscosity to be $\nu_0/2$.

$$\bar{\nu}(z) = \nu_V \chi_V(z) + \nu_L[1 - \chi_V(z)] = \nu_L - \chi_V(z)[\nu_L - \nu_V] \tag{11}$$

### B. Criterion

The criterion to satisfy in order to enable the vapor slug expansion is given by Eq. (12). When, it is expressed using the inlet control parameters (the heat flux $Q_W$, the liquid inlet velocity $U_0$), we obtain:

$$\frac{\alpha L \nu_0 \varrho_m U_m}{2\varrho_0 U_0^2 D_H^2} > K_1 \tag{12}$$

$$\frac{Q_W}{U_0^2} > K_1 \frac{4\varrho_0 A_H L_V D_H^2}{\alpha \nu_0 \delta L^2} \tag{13}$$

Equation (13) threshold will be named $K_2$ in further calculations. The relation between $K_1$ and $K_2$ is given by Eq. (14) which does only depend on physical and geometric parameters. A numerical application gives the ratio $K_1/K_2 = 3.92 \times 10^{-6}\ \text{s} \cdot \text{m}^2 \cdot \text{Kg}^{-1}$ $\pm 7.5\%$. The threshold uncertainty is only due to the minichannel hydraulic diameter uncertainty

$$\frac{K_2}{K_1} = \frac{\alpha \nu_0 \delta L^2}{4\varrho_0 A_H L_V D_H^2} \tag{14}$$

This theoretical threshold allows one to link the critical pressure loss to a critical heat flux through Eq. (15). It exists a critical pressure loss for a given heat flux, fluid, and geometry which destabilize the two-phase flow. For our study, the ratio given Eq. (15) is $1.23 \times 10^{-3}\ \text{s} \cdot \text{m}^{-1}$.

$$\frac{\Delta P^c_{\text{minichannel}}}{Q^c_w} = \frac{\varrho_0}{2}\frac{K_2}{K_1} = \frac{\alpha \nu_0 \delta L^2}{8A_H L_V D_H^2} \tag{15}$$

## IV. Flow Stability and Scaling Laws

### A. Experimental Stability Criterion

In a previous paper, we presented experimental exit vapor quality ($\chi_v^{\text{out}}$) obtain for five different heat fluxes (Fig. 10 in [21]). On this figure a transition criteria appear for all heat fluxes and is materialized by a dash line [$\chi^c = f(Re^c)$]. Thereby, a marginal stability line can be proposed. Thus, a linear relation between the critical exit vapor quality and the critical inlet Reynolds number is proposed [Eq. (16)], using the exit vapor quality definition with the phase change number [($N_{\text{pch}}$ in Eq. (17)] and the subcooling number [($N_{\text{sub}}$ in Eq. (18)].

$$\chi_v^{\text{out}} = N_{\text{pch}} - N_{\text{sub}} = A\, Re^c \tag{16}$$

$$N_{\text{pch}} = \frac{4q_W}{\varrho_0 U_0 L_V}\frac{L}{D_H} \tag{17}$$

$$N_{\text{sub}} = \frac{\Delta h_i}{L_V} \tag{18}$$

In Eq. (16), $Re^c$ and $\chi^c_{\text{out}}$ are related using a constant A. For all Reynolds numbers above this critical value, convective boiling is steady whatever is the heat flux, whereas above this critical value convective boiling is unsteady. So, flow boiling stability can be characterized by the ratio $(N^c_{\text{pch}} - N^c_{\text{sub}})/Re^c$. The constant A differs

as a function of the inlet conditions. The unsteady states are all located in the first part of the curve: pressure loss function of inlet Reynolds number. The objective is using the analysis previously detailed
to find a common way to express all the experimental results to analyze the physical mechanisms of heat and mass transfer in the minichannel.

### B. Pressure Loss Scaling Law

Figure 6 of Brutin and Tadrist [21] presents the total minichannel pressure loss as a function of the inlet Reynolds number. The total pressure loss includes the liquid, two-phase and vapor depending of the boiling stage in the minichannel. The curve behavior in *N* shape is observed for all the heat fluxes studied. The total minichannel pressure loss which is the sum of fluid pressure loss by zones and arise when the friction term in the two-phase zone is maximum then decreases corresponding to a flow mainly vapor. With the increasing heat fluxes, the pressure loss shift for higher values and the *N* shape is more and more pronounced. Using the experimental results of the previous section, it is possible to propose a global behavior of the fluid flow in the minichannel with the nondimensioned pressure loss variation. If we remove all points that present liquid flow operating conditions and those for mainly vapor flow in the minichannel, we obtain only the operating condition which satisfies the exit vapor quality in strictly in between 0 and 1 (Fig. 6). Two cases are studied: the "confinement case" with a constant mass flow rate provided to the channel entrance and the "compliant case." This last one is studied to introduce inlet pressure fluctuations using a buffer thank. All the results on the pressure loss are only one line which means a same variation law. Equation (19) provides numerically the pressure loss scaling law. It is also possible from Fig. 6 to extract the transition criteria from steady to unsteady. This law provides an equivalent friction factor for the two-phase flow.

$$\Delta P^*_{\text{comp}} = 4.4 \times 10^4 \left(\frac{N_{\text{pch}}}{Re_0}\right)^{0.818} \tag{19}$$

Figure 6 evidences a possible generalization of the steady and unsteady results. The stability transition appears for a given abscissa and thus a given ordinate. These coordinates are summarized by the ratio $K_2/K_1$ previously detailed with Eq. (14). The experimental values of $K_2/K_1$ are given in Table 2 with a comparison to the theoretical ones. We obtain a good agreement between the experimental threshold and the theoretical one. For the coupling case a gap of 14 and 26% for the confinement case compared with the total

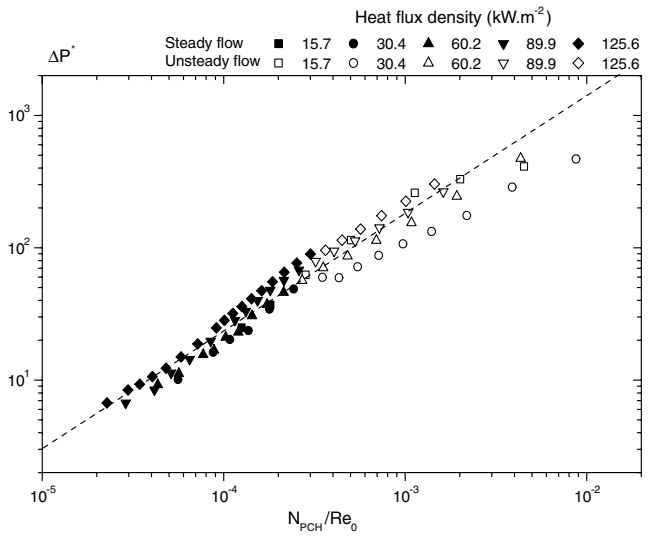


**Fig. 6 Pressure loss scaling law for all heat flux densities provided: nondimensioned pressure loss function of the ratio between the phase change number and the Reynolds one for only exit vapor qualities in between 0 and 1 excluded.**

**Table 2 Experimental and theoretical determination on the two-phase flow destabilization threshold (unit: $s \cdot m^2 \cdot Kg^{-1}$) for both flow inlet situations**

| Case | Experimental threshold | Theoretical threshold | Exp-Th. Gap |
|---|---|---|---|
| Coupling | $4.48 \times 10^{-6} \pm 30\%$ | $3.92 \times 10^{-6} \pm 7.5\%$ | 14% |
| Confinement | $4.94 \times 10^{-6} \pm 30\%$ | $3.92 \times 10^{-6} \pm 7.5\%$ | 26% |

uncertainty of 37.5% due to the experimental and theoretical destabilization threshold determination [Eqs. (20) and (21)] complexity with uses 4 times the liquid inlet velocity, 4 times the hydraulic diameter, the total pressure drop, the heat flux

$$\Delta P^* = \frac{\Delta P}{\frac{1}{2}\varrho_0 U_0^2} \tag{20}$$

$$\frac{N_{\text{pch}}}{\text{Re}_0} = \frac{Q_W}{U_0^2}\frac{4L\nu_0}{\varrho_0 D_H^2} \tag{21}$$

### C. Oscillation Frequency Scaling Law

The two-phase flow oscillation frequencies observed can also be analyzed using a nondimensional approach. Their experimental values are obtained based on the pressure drop fast Fourier transformation which evidence frequencies of high energy. The fundamental is the frequency we deal with here. The oscillation mechanism is based on the two-phase transport along the minichannel, it is mainly a convective phenomenon which drives pressure oscillations. Thus, the convective time ($\tau$) defined in Eq. (22) is used.

$$\tau = \frac{L}{U_0} \tag{22}$$

The nondimensional two-phase flow frequency ($F \cdot \tau$) is plotted as a function of ($N_{\text{pch}}/Re_0$). A unique curve is found for all the operating conditions. This behavior confirms that the oscillation frequency is mainly driven by the phase change phenomena and inertia effects (Fig. 7). The dispersion is probably due to the uncertainty associated with the frequency measurement.

### D. Heat Transfer Coefficient Scaling Law

The heat transfer coefficient calculated here is based on the average surface and fluid temperature. A total heat flux is provided ($\bar{Q}_W$) whereas locally the heat flux redistributes inside the aluminum rod. Thus, the local surface and fluid temperatures cannot be used to

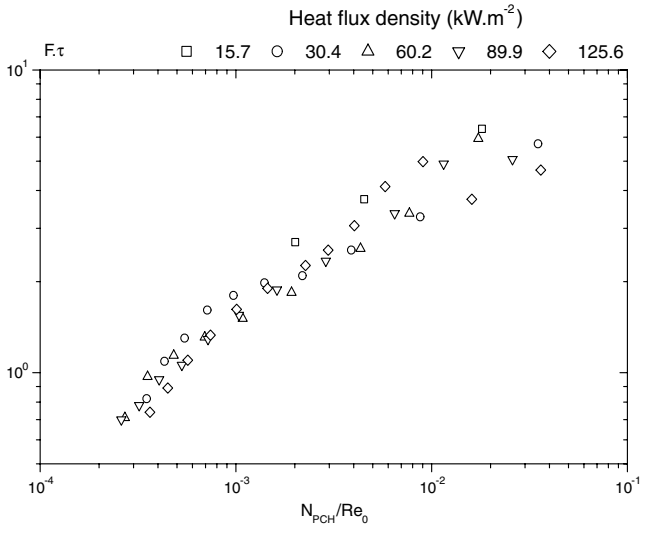


**Fig. 7 Nondimensioned oscillation frequency function of $N_{\text{pch}}/Re_0$.**

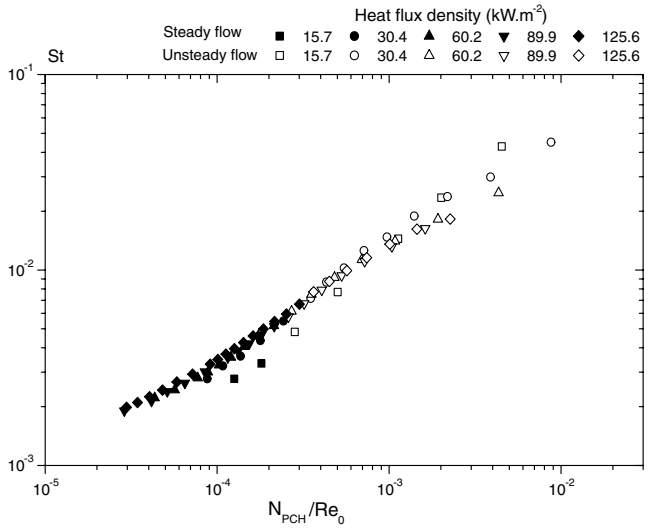


**Fig. 8 Heat transfer scaling law for all heat flux densities studies and exit vapor qualities in between 0 and 1 excluded.**

calculate a local heat transfer coefficient but can provide only a global heat transfer coefficient. Using the average temperature difference between surface and fluid ($\bar{T}_S - \bar{T}_F$) and the total heat flux transferred to the fluid, we calculate a global heat transfer coefficient [Eq. (23)]. We presented with Fig. 12 of [21] only operating conditions which correspond to a two-phase zone in the minichannel are considered. The objective is to analyze the two-phase flow contribution on heat transfer.

For increasing heat fluxes, the $N$ shape is more and more pronounced. Dark points on Fig. 12 of [21] represent a steady flow, whereas the white points are for an unsteady flow. A mean heat transfer coefficient is deduced. Introducing the Stanton number, we compare the heat flux transferred to the fluid to the heat transported with the fluid. If we consider only the operating conditions which satisfy a two-phase zone mainly in the minichannel (Fig. 8); it appears a heat transfer scaling law [Eq. (25)]. Thus, it is possible to predict a mean heat transfer coefficient when a two-phase zone is mainly inside the minichannel.

$$\bar{h} = \frac{\bar{Q}_W}{\bar{T}_S - \bar{T}_F} \tag{23}$$

$$\mathrm{St} = \frac{\bar{h}}{\varrho_0 C p_0 U_0} \tag{24}$$

$$\mathrm{St} = 0.776\left(\frac{N_{\mathrm{pch}}}{Re_0}\right)^{0.589} \tag{25}$$

## V. Conclusion

We developed a model based on a vapor slug expansion. A critical nondimensioned number is found to characterize the flow stability transition. This theoretical criteria is in good agreement with experimental values. This model based on the flow pattern observation allows one to explain the onset of the unsteady state. Based on this criterion we proposed pressure loss, heat transfer, and oscillation frequency scaling laws. This characteristics number allows to analyze quite well the experimental results. It evidences the coupling phenomena between the liquid–vapor phase change and the inertia effects.

## Acknowledgment

We thank the "Centre National d'Études Spatiales" for its financial assistance Grant No. 793/2002/CNES/8665.

## References

[1] Kandlikar, S. G., "Fundamental Issues Related to Flow Boiling in Minichannels and Microchannels," *Experimental Heat Transfer, Fluid Mechanics, and Thermodynamics, ExHFT-5*, Vol. 1, Edizioni ETS, Pisa, Sept. 2001, pp. 129–146.

[2] Kandlikar, S. G., "Heat Transfer Mechanisms During Flow Boiling in Microchannels," *Journal of Heat Transfer*, Vol. 126, 2004, pp. 8–16.

[3] Steinke, M., and Kandlikar, S., "An Experimental Investigation of Flow Boiling Characteristics of Water in Parallel Microchannels," *Journal of Heat Transfer*, Vol. 126, No. 4, 2004, pp. 518–526.

[4] Stenning, A. H., and Veziroglu, T. N., "Flow Oscillation Modes in Forced Convection Boiling," *Proceedings of the Heat Transfer and Fluid Mechanics Institute*, 1965, pp. 301–316.

[5] Davies, A. L., and Potter, R., "Hydraulic Stability: An Analysis of the Causes of Unstable Flow in Parallel Channels," *Proceedings of the Symposium on Two-Phase Flow Dynamics*, 1967, pp. 1225–1266.

[6] Bouré, J. A., Bergles, A. E., and Tong, L. S., "Review of Two-Phase Flow Instability," *Nuclear Engineering and Design*, Vol. 25, 1973, pp. 165–192.

[7] Bergles, A. E., "Review of Instabilities in Two-Phase Systems," *Two-Phase Flows and Heat Transfer*, NATO Advanced Study Institute, Istanbul, 1976, pp. 383–423.

[8] Blum, J., Marquard, W., and Auracher, H., "Stability of Boiling Systems," *International Journal of Heat and Mass Transfer*, Vol. 39, No. 14, 1996, pp. 3021–3033.

[9] Kew, P. A., and Cornwell, K., "On Pressure Fluctuations During Boiling in Narrow Channels," *Proceedings of the 2nd European Thermal-Sciences and 14th UIT National Heat Transfer Conference*, 1996, pp. 1323–1327.

[10] Chang, S. H., Kim, Y. I., and Baek, W.-P., "Derivation of Mechanistic Critical Heat Flux Model of Water Based on Flow Instabilities," *International Communications in Heat and Mass Transfer*, Vol. 23, No. 8, 1996, pp. 1109–1119.

[11] Umekawa, H., Ozawa, M., Miyazaki, A., Mishima, K., and Hibiki, T., "Dryout in a Boiling Channel under Oscillatory Flow Condition," *JSME International Journal, Series B (Fluids and Thermal Engineering)*, Vol. 39, No. 2, 1996, pp. 412–418.

[12] Yan, Y., and Kenning, D. B. R., "Pressure Fluctuations During Boiling in a Narrow Channel," *HTFS Research Symposium*, 1998.

[13] Kim, Y. I., Baek, W.-P., and Chang, S. H., "Critical Heat Flux Under Flow Oscillation of Water at Low-Pressure, Low-Flow Conditions," *Nuclear Engineering and Design*, Vol. 193, 1999, pp. 131–143.

[14] Roach, G. M., Abdel-Khalik, S. I., Ghiaasiaan, S. M., Dowling, M. F., and Jeter, S. M., "Low-Flow Onset of Flow Instability in Heated Microchannels," *Nuclear Science and Engineering*, Vol. 133, 1999, pp. 106–117.

[15] Kennedy, J. E., Roach, G. M., Dowling, M. F., Abdel-Khalik, S. I., Ghiaasiaan, S. M., Jeter, S. M., and Quershi, Z. H., "The Onset of Flow Instability in Uniformly Heated Horizontal Microchannels," *Journal of Heat Transfer*, Vol. 122, February 2000, pp. 118–125.

[16] Babelli, I., and Ishii, M., "Flow Excursion Instability in Downward Flow Systems. Part 2: Two-Phase Instability," *Nuclear Engineering and Design*, Vol. 206, 2001, pp. 97–104.

[17] Peles, Y. P., Yarin, L. P., and Hestroni, G., "Steady and Unsteady Flow in a Heated Capillary," *International Journal of Multiphase Flow*, Vol. 27, 2001, pp. 577–598.

[18] Qu, W., and Mudawar, I., "Measurement and Prediction of Pressure Drop in Two-Phase Micro-Channels Heat Sinks," *International Journal of Heat and Mass Transfer*, Vol. 46, 2003, pp. 2737–2753.

[19] Li, H. Y., Lee, P. C., Tseng, F. G., and Pan, C., "Two-Phase Flow Instability of Boiling in a Double Microchannel System at High Heating Powers," *Proceedings of the 1st International Conference on Microchannels and Minichannels*, American Society of Mechanical Engineers, Fairfield, NJ, 2003, pp. 615–621.

[20] Brutin, D., Topin, F., and Tadrist, L., "Experimental Study of Unsteady Convective Boiling in Heated Minichannels," *International Journal of Heat and Mass Transfer*, Vol. 46, No. 16, 2003, pp. 2957–2965.

[21] Brutin, D., and Tadrist, L., "Pressure Drop and Heat Transfer Analysis on Flow Boiling in a Minichannel: Influence of the Inlet Condition on Two-Phase Flow Stability," *International Journal of Heat and Mass Transfer*, Vol. 47, No. 10–11, 2004, pp. 2365–2377.

[22] Fritz, W., "Maximum Volume of Vapor Bubbles," *Physikalische Zeitschrift*, Vol. 36, 1935, p. 379.

[23] Brutin, D., "Écoulements Liquides en Microtubes et Ébullition Convective en Minicanaux : Étude Expérimentale et Modélisation," Ph. D. Thesis, Université d'Aix–Marseille I, Marseilles, France, October 2003.